Implementation and Evaluation of a Gigabit Ethernet FSO Link for 'The Last Metre and Last Mile Access Network'

Mojtaba Mansour Abadi[1], Zabih Ghassemlooy[1], Nithin Mohan[1], Stanislav Zvanovec[2], Manav R. Bhatnagar[3], Ralph Hudson[4]

[1] Optical Communications Research Group, Faculty of Engineering and Environment, Northumbria University, Newcastle upon Tyne, UK; (mojtaba.mansour, z.ghassemlooy, nithin.mohan)@northumbria.ac.uk

[2] Department of Electromagnetic Field, Faculty of Electrical Engineering, Czech Technical University in Prague, Technicka 2, Prague 16627, Czech Republic; (e-mail: xzvanove@fel.cvut.cz)

[3] Department of Electrical Engineering, Indian Institute of Technology Delhi, New Delhi 110016, India; (email: manav@ee.iitd.ac.in)

[4] The Core, Bath Lane, Newcastle Helix, Newcastle upon Tyne, NE4 5TF

***Abstract*— In this paper, we propose a simple and a lost cost 1 Gbps Ethernet free-space optical (FSO) communications link, which can be used both for the last meter and last mile access networks. In the emerging fifth generation wireless systems, which require at least an order of magnitude increase in the peak data rates and three orders of magnitude increase in network capacity with reduced latency, deploying multiple technologies will play a crucial role to meet these requirements. One possible complementary wireless technology to the radio frequency is the unlicensed FSO, which can bridge the gap between the existing RF wireless and optical fibre communication networks by providing high data rates, low installation costs and high energy efficiency. In this work, we propose a high-speed FSO system, which can be readily implemented using off the shelf components, and assess its performance experimentally under turbulence and fog conditions using the dedicated indoor atmospheric chamber. We show that, the proposed system under the turbulence condition with a scintillation index of 0.43 offers almost the same data rate (i.e., ~99%) as the link under a clear channel, while the packet-error-rate reduces from 10^{-3} to 2×10^{-2}.**

Keywords*— *Gigabit Ethernet, FSO, Turbulence, Fog

I. INTRODUCTION

Free space optics (FSO) as part of the optical wireless communications (OWC) is seen as an attractive technology with application in a number of areas, where the radio frequency (RF) based wireless technologies cannot provide the required bandwidth [1]. FSO can bridge the gap between the back-bone optical fibre (OF) communications and RF wireless networks (WNs) by providing a high data rates R_b using the massive licence free spectrum (up to ≅ 400 THz), inherent security at the physical layer due to small optical footprints, low installation costs, reduced latency and high energy efficiency (as part the global green telecommunications agenda). In macro- and micro-cells high-speed FSO transceivers (i.e., base-stations) with beam steering capabilities could be deployed as part of back- and front-haul traffic in places, where deployment of optical fibre and cable-based fixed links are not economical. In next generation WNs (i.e., 5G and beyond), it is envisaged that FSO (both visible and infrared bands) will also play a role as part of the smart applications requiring a very high R_b [2]. In particular, in the last metre and last miles access networks, as illustrated in Fig. 1, FSO is seen as a potential solution to address the bandwidth

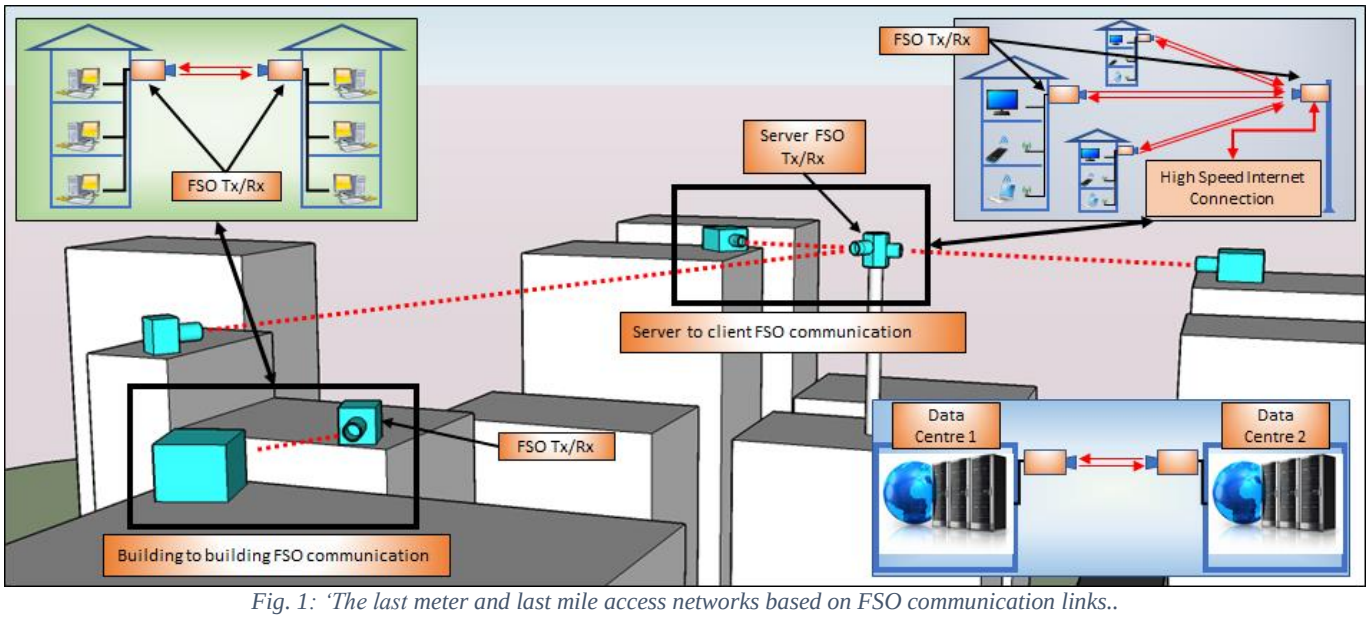

Fig. 1: 'The last meter and last mile access networks based on FSO communication links..

bottleneck [3] by offering high R_b of > 1 Gbps over transmission distances up to a few kms [1].

For the end-user's applications, R_b of a few Gbps is adequate to cope with the planned targets. For instance, in the united kingdom (the UK), buildings are expected to be connected to the internet using Gigabit OF to the home broadband technology by 2025 [4]. However, the price of OF installation, geographical constraints, and services availability make OF to the home target quite challenging to meet. Therefore, in such situations, the FSO technology can be good candidate to provide services temporarily or even permanently. Commercial FSO systems typically operate at R_b of $\leq$ 10 Gbps and can reach a range of up to 1.5 km and 30 Gbps systems are beginning to appear in the market. A number of research works demonstrating the potential for Tbps transmission using space division multiplexing and orbital angular momentum schemes have been reported [5, 6], which are costly and complex.

As for the last meter and last mile access WNs, the FSO technology needs to be cost effective and less complex using the readily available components and devices with acceptable performance. In this paper, we present a 1 Gbps Ethernet FSO system based on using the off-of-shelf components, which can be used in both last meter and last mile access WNs and can readily be connected to the back-bone OF networks. The proposed architecture is cost effective, robust and easily assembled. We present the system concept, outline the develop experimental FSO link and investigate its performance under various atmospheric conditions using the dedicated indoor atmospheric chamber. We show that, the proposed system under turbulence offers almost the same data rate (i.e., ~99%) as a clear channel, while the packet-error-rate is downgraded from 10^{-3} to 2×10^{-2}.

The paper is organized as follows. Section 2 describes the FSO system and provide basic design considerations. Section 3 presents the results and discussion on the measured data. Finally, Section 4 concludes the paper.

II. FSO System Design

The schematic block diagram of the proposed full duplex system is presented in Fig. 2, which is simple and uses the off-the-shelf components. The FSO transceiver unit utilizes a media convertor (MC) module and a small form-factor pluggable transceiver (SFP) for converting 1 Gbps Ethernet into optical signal for transmission over a single mode fibre SMF) and vice-versa. The transmit (Tx) output of SFP optics composed of an adjustable lens and an expander (i.e., a concave lens) is used to launch the light emerging from the SMF into the free space channel. Note that the lens and expander are used for changing the beam divergence and to expand the beam prior to transmission over the channel.

At the receiver (Rx) a telescope, which is a combination of an objective lens, an eyepiece, an optical bandpass filter, and a fibre port, is used to couple the incoming light into a multi-mode fibre (MMF). The objective and eyepiece lenses are separated by both focal lengths added up. Ideally, the fibre port should be as close as possible to the eyepiece lens. However, it is better to leave a gap between to make the alignment process easier. To reduce the effect of the ambient light, it is a good practice to filter out the unwanted light using an optical bandpass filter, see Fig. 2. The output of the MMF is applied to the SFP-MC module for conversion back to the electrical 1Gbps Ethernet signal. Since the system is a full duplex, the same configuration is adopted for both paths.

A commercially available SFP has a typical optical output power of < 2 dBm whilst the minimum required power at the Rx to support 1 Gbps is > -14 dBm, which allows a total link loss of ~16 dB.

The total link loss in dB is given as [7]:

$$A_{tot} = 20\log_{10}\left[\frac{\sqrt{2}(w_0+L\theta)}{D_{Rx}}\right] + A_{misc}, \quad (1)$$

where w_0, θ, L, and D_{Rx} denote the radius and half-angle divergence angle of the beam emerging from Tx, link length, and the Rx's aperture diameter (diameter of objective lens in Fig. 2), respectively. Note, the first term in (1) is the geometrical loss whereas A_{misc} refers to other losses due to misalignment and optics. In an ideal FSO system the optical beam is collimated and is narrow in order to minimize the propagation loss. Here, the optical beam is expanded for a number of reasons including (*i*) alignment, since the size of the optical illumination area is orders of magnitude higher

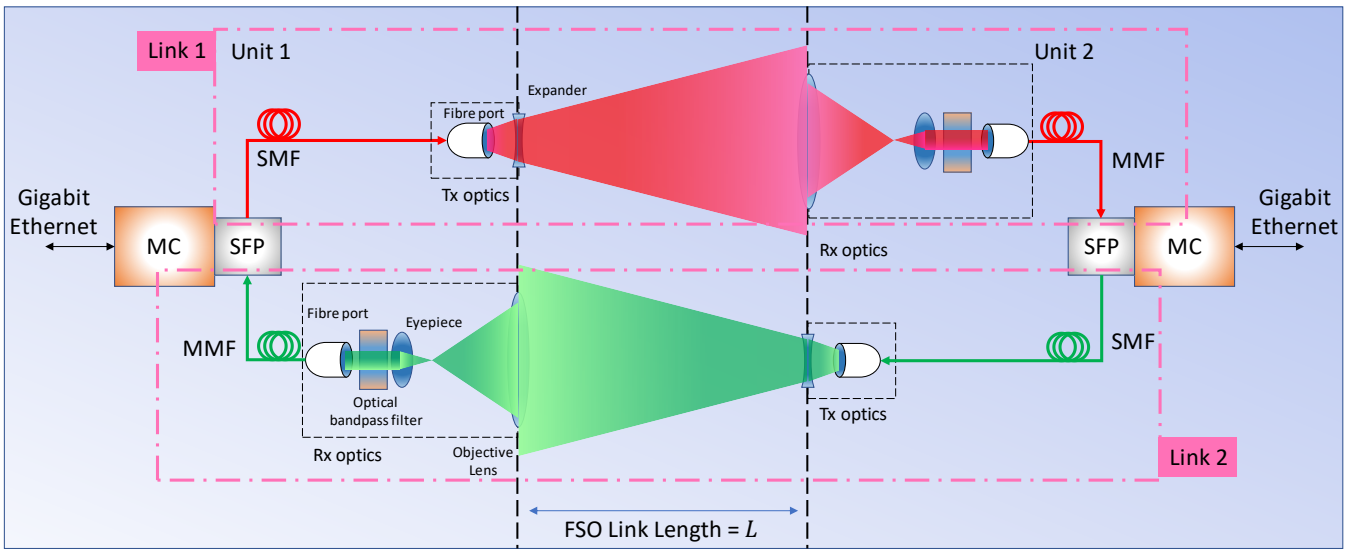

Fig. 2: A schematic block diagram of the Gigabit Ethernet FSO link. MC, SFP, SMF, and MMF denote media convertor, small form-factor pluggable transceiver, single mode fibre, and multimode fibre, respectively. Link 1 and 2 are marked with a pink dash-dot boxes.

than Rx aperture surface area; (*ii*) meet the eye safety power requirement; and (*iii*) immunity against channel effects. However, the disadvantage of beam expansion is the reduced power level at the Rx, thus the need for high-sensitivity photodetector (PD) or reduced transmission range to ensure quality of services.

As for the eye safety, the laser used needs to be Class 1M, which must meet the following condition [8]:

$$\frac{P_{Tx}}{P_{AEL}} < 1 - e^{-\left(\frac{d_a}{d_{63}}\right)^2}, \quad (2)$$

where P_{Tx} and P_{AEL} are transmit optical power and the maximum accessible emission limit (AEL) power for Class 3B laser, respectively. d_a is the aperture stop specified by the laser eye safety standard for a given distance and d_{63} is the beam diameter at 63% of the total power. Given that, for the aperture stop of 7 mm the required distance is 14 mm, then $d_{63} = 2 \times (w_0 + 14 \times 10^{-3}\theta)$ As we outlined earlier, an FSO link with the divergent beam is less susceptible to the channel effects particularly the pointing errors [1, 2]. This is because the beam radius w is much larger than the Rx's aperture radius. Further, we need to avoid too wide beam sizes due to geometrical loss and minimum required power at Rx. The beam intensity variation due to the pointing errors is given by [9]:

$$\mathrm{V}_{PE} = \frac{A_0^2\gamma^2}{2+\gamma^2} - \frac{A_0^2\gamma^4}{(1+\gamma^2)^2}, \quad (3)$$

where A_0 corresponds to the geometrical loss, $\gamma = w_{\mathrm{eq}}/2\sigma_j$, and σ_j^2 is the jitter variance. We have $A_0 = [\mathrm{erf}(v)]^2$ and $w_{\mathrm{eq}}^2 = w^2\frac{\sqrt{\pi}\mathrm{erf}(v)}{2v\exp(-v^2)}$ where $v = \sqrt{\pi/2}\frac{a}{w}$ and $\mathrm{erf}(x) = \frac{2}{\sqrt{\pi}}\int_0^x e^{-t^2}dt$. Based on the given variance expression it can be shown that, for a beam radius at least twice that of the Rx aperture radius, the received signal variance is less than 1% even for the extreme condition of $\sigma_j^2 = 1$.

The minimum size of the Rx aperture is determined by either the minimum required received power at the Rx, cf. (1), or the maximum tolerable turbulence level. The aperture averaging reduces the fading effect. Knowing the Rx aperture size and the beam wavelength λ under turbulence conditions, the aperture averaging is given by [10]:

$$\mathrm{AF} = \frac{\sigma_I^2(d_s)}{\sigma_I^2(0)} \approx \left[1 + 1.6682\left(\frac{D_{Rx}}{\sqrt{\lambda L}}\right)^2\right]^{-7/6}, \quad (4)$$

where $\sigma_I^2(D_{Rx})$ and $\sigma_I^2(0)$ are the normalised variance of the received signal or scintillation index with and without apertures, respectively. Turbulence is classified into weak ($\sigma_I^2 < 1$), moderate ($\sigma_I^2 \cong 1$) and strong ($\sigma_I^2 \gg 1$) depending on the scintillation index value. For weak turbulence σ_I^2 is given by [11]:

$$\sigma_I^2 = 1.23\left(\frac{2\pi}{\lambda}\right)^{\frac{7}{6}} C_n^2 L^{\frac{11}{6}}, \quad (5)$$

where C_n^2 the refractive index structure coefficient of the channel. C_n^2 can be either directly measured from the channel environmental parameters such as temperature and pressure, or calculated from different models. It can vary from $1.7 \times 10^{-14}\ m^{-2/3}$ during daytime to $8.4 \times 10^{-15}\ m^{-2/3}$ at night for terrestrial FSO links [11].

For a slow-fading channel with OOK, the signal-to-noise ratio (SNR) at the Rx is defined as:

Table 1: Parameters and specification of the system presented in Fig. 2.

	Parameter	Value
Given	D_{Rx}	75 mm
	L	500 m
	C_n^2	10^{-13} m$^{-2/3}$
Calculated	θ	0.5 Deg
	Geometrical Loss	9 dB
	Minimum required D_{Rx}	40 mm
	Maximum eye safe power for Class 1M	~27 dBm
	Rytov variance of tolerable turbulence (10% criteria)	0.6
Other	Eyepiece diameter	25. 4 mm
	Eyepiece focal length	25 mm
	Objective diameter	75 mm
	Objective focal length	150 mm
	w_0	1.5 mm
	Fibre port focal length	4.6 mm
	Fibre port diameter	10 mm
	Optical filter passband	1510 to 1590 nm
	SFP output power	~2 dBm
	SFP sensitivity	−23 dBm
	SFP wavelength	1550 dBm

$$SNR(h) = \frac{2P_t^2R^2h^2}{\sigma_n^2}, \quad (6)$$

where P_t is the average transmit power, h is the channel transfer function, R is the PD responsivity (in A/W) and σ_n^2 is the additive white Gaussian noise variance. Note, noise arises from various sources such as the shot noise caused by the signal itself and/or ambient light, dark current noise, and electrical thermal noise. Assuming the maximum normalized variance due to turbulence for a given Rx aperture diameter is 10%, the minimum Rx aperture size is derived from (4) and (5) as:

$$D_{Rx} > \sqrt{32.37 \times C_n^{2\frac{6}{7}} \times L^{\frac{18}{7}} - \frac{\lambda L}{1.67}}, \quad (7)$$

As for the optics, we have used a 75 mm diameter aperture at the Rx, which makes the system immune to turbulence with $\sigma_I^2 = 0.6$ for a link span of 500 m and for C_n^2 of 10^{-13} m$^{-2/3}$ (i.e., strong turbulence) [11]. The eye safety regulation classifies the laser as Class 1M, which is conditionally safe. However, in this work the laser power is set to be < 10 mW hence making the laser beam Class 1 and unconditionally safe. Thus, for the proposed system with the SFP output power of < 2 dBm, the laser output power level is within the eye safe limit. All the key system parameters and specifications are summarised in Table 1. The eyepiece lens parameters are based on the commercially available lens.

III. Results and Discussions

To perform the experiment, we used the Link 1 in Fig. 2 and replaced Link 2 with a fibre connection. Note, the Link 2 can also be based on FSO. The experimental setup shown in Fig. 4 was used to assess the performance of the proposed system under different channel conditions. The SFP is a MSA Compliant SFP Transceiver Module - 1000BASE-ZX, while we used a TP-Link MC220L Fibre media converter. The 1 Gbps Ethernet connection was aligned over a 7.2 m long atmospheric chamber while a fibre connection was provided to close the Tx/Rx loop. Turbulence was generated using hot

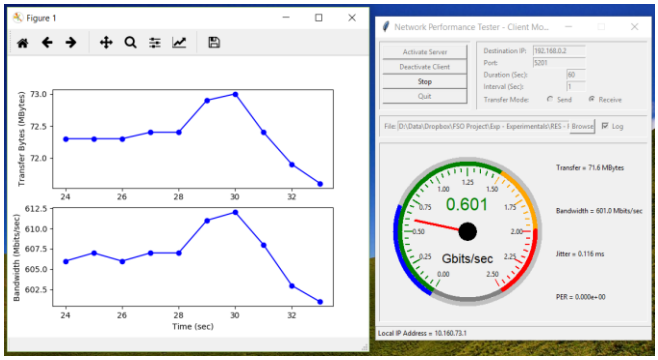

of the developed python code for measuring the performance of the

and cool fans injected into the chamber. The temperature profile within the chamber was monitored using 17 distributed temperature sensors position at a spacing of ~25 cm along the chamber. The measured temperatures were also used to estimate C_n^2 within the chamber [12]. In addition, a Rx was used at one end of the chamber to capture a red laser modulated with non-return-to-zero on-off keying NRZ-OOK signal transmitted from the other end. We used the method described in [12] to estimate the effect of turbulence on the signal in terms of scintillation index σ_I^2. A green laser and a power meter were utilized to measure the visibility $V = \frac{3.91}{\sigma}\left(\frac{\lambda}{550}\right)^{-q_s}$ within the chamber under fog condition based on the method outlined in [13, 14]. The quality of the Ethernet connection was assessed using the python tool, which we developed based on an open source tool known as *iperf* [15], see Fig. 3. This tool provides important parameters including achieved R_b, jitter and packet error rate (PER) (i.e., packet loss). Note, σ is the attenuation coefficient and q_s is a parameter related to the particle size distribution and V as defined in [13, 14]. We carried out a set of measurements, each lasting over 1 minute with a sampling interval of 1 second whilst an average of 14500 datagrams were transmitted each second. The maximum achievable R_b of MC and SFP modules and *iperf* tool was tested for the back-to-

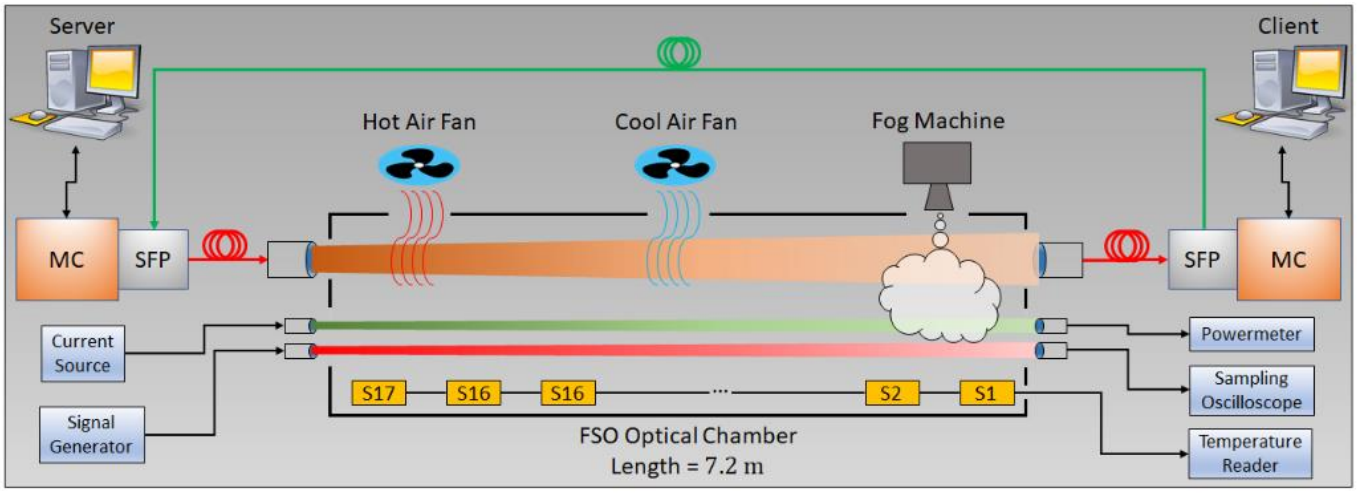

(a)

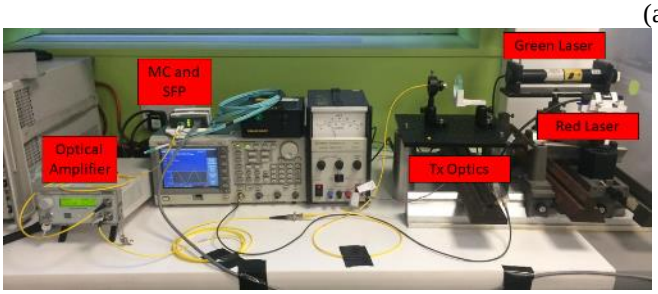

(b)

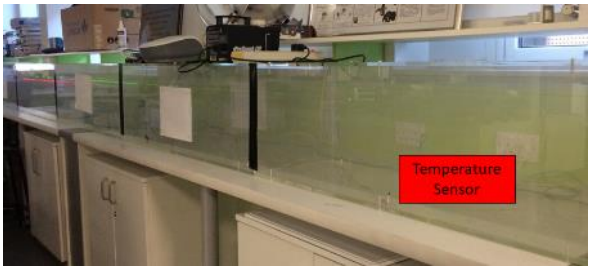

(c)

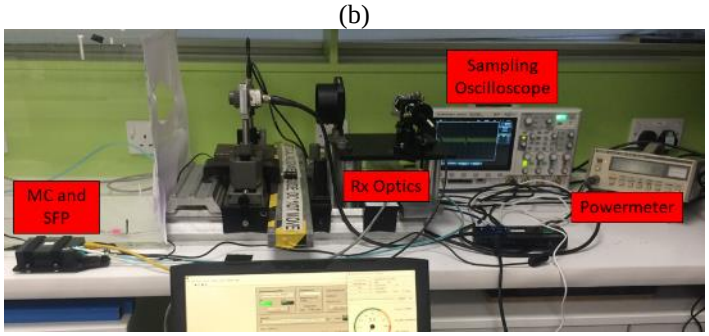

(d)

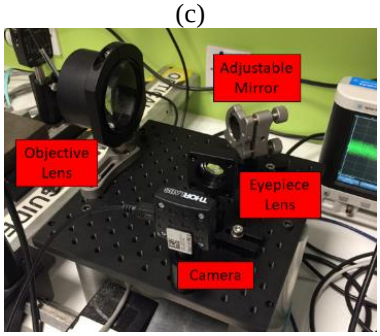

(e)

Fig. 3:a) Block diagram of the experimental setup. MC and SFP denote media convertor and small form-factor pluggable transceiver. S_i is the temperature sensor mounted inside the chamber. b) transmitter setup where green and red lasers are used to measure the visibility and scintillation index of the channel, respectively. c) channel setup with a labelled temperature sensor. d) Rx setup where sampling oscilloscope and powermeter are used to measure turbulence stregth and visibility in the atmospheric chamber. and e) camera setup where the fibre port is replaced with a camera. The mirror is used for adjusting the focused beam on camera image sensor.

Table 2: Parameters and specification of the system presented in Fig. 2. PER, C_n^2, and σ_I^2 denote packet-error-rate, the refractive index structure coefficient, and the scintillation index, respectively.

Channel condition	Parameter	Mean value	Standard deviation	Minimum	Maximum
B2B	Data rate (Mbps)	602.70	5.47	587.00	608.00
	Jitter (µs)	109.37	11.60	86.00	133.00
	PER	6.55×10^{-4}	4.06×10^{-3}	0.0	3.03×10^{-2}
Clear	Data rate (Mbps)	601.03	6.34	586.00	608.00
	Jitter (µs)	101.36	9.42	85.00	130.00
	PER	9.90×10^{-4}	4.1×10^{-3}	0.0	3.01×10^{-2}
Fog, Visibility = 8.04 m	Data rate (Mbps)	95.72	0.28	94.70	97.00
	Jitter (ms)	22.42	130.53	0.18	950.27
	PER	2.51×10^{-3}	3.82×10^{-3}	0.0	2.37×10^{-2}
Fog, Visibility = 34.04 m	Data rate (Mbps)	606.41	7.56	581.00	613.00
	Jitter (µs)	108.36	19.46	84.00	229.00
	PER	4.36×10^{-3}	4.99×10^{-3}	0.0	3.40×10^{-2}
Turbulent, $C_n^2 = 6.39\times10^{-11}$ m$^{-2/3}$, $\sigma_I^2 = 0.10$	Data rate (Mbps)	594.20	22.09	504.00	613.00
	Jitter (ms)	0.51	3.02	0.09	23.30
	PER	2.12×10^{-2}	3.24×10^{-2}	1.07×10^{-4}	1.39×10^{-1}
Turbulent, $C_n^2 = 2.22\times10^{-10}$ m$^{-2/3}$, $\sigma_I^2 = 0.43$	Data rate (Mbps)	595.98	19.19	522.00	612.00
	Jitter (ms)	2.34	13.40	0.08	101.26
	PER	2.23×10^{-2}	3.14×10^{-2}	2.15×10^{-4}	1.46×10^{-1}

back (B2B) server and client link, see Table 2. The maximum R_b achievable with the proposed link was almost 602 Mbps with a PER of 6.55×10^{-4}, which was limited by the hardware specifications.

Next, we performed measurements under different channel conditions of clear, with fog and turbulence. Since in the clear chamber the propagating optical signal only experiences attenuation the link performance is not severely affected, cf. Table 2. Considering a geometrical loss given in Table 1, the 7 dB link margin is sufficient to compensate for the fog induced attenuation. Therefore, for a 500 m long link span, the minimum V range is 2.35 km. In this work, we reduced V, which resulted in a 5 dB of attenuation within the chamber, and consequently R_b dropped to 100 Mbps with a PER of 2.51×10^{-3}. Note that, the high reduction in R_b, which is expected since signal-to-noise ratio (SNR) is reduced, was managed by using the server and the client operating system automatically. By increasing V to 34 m i.e., reducing the channel loss to 1.2 dB, R_b increased to 600 Mbps. With turbulence, R_b remained almost intact, however both the jitter and PER increased. For a given Tx aperture size, see Table 1, the scintillation index of 0.43 droped down to 0.04, which is tolerated by the SFP module and hence no significant dropdown in the measured average R_b. However due to randomness of the channel condition, the overall PER and jitter were worse than the clear channel as expected.

As seen from the measurement results, provided the conditions in section 2 are satisfied the average R_b for the link is the same as the B2B link, cf. Table 2. However, note that the additional loss A_{misc} in (1) is kept to a minimum level. Based on our observations from the experimental measurements we noted that, three sources for the additional losses incurred in the proposed FSO system: (*i*) beam clipping due to the optics at the Tx and the Rx; (*ii*) light coupling efficiency from free space to the OF at the Rx optics; and (*iii*) light coupling efficiency from OF to the PD at the Rx SFP. Based on the measured optical link power budget, beam clipping at Tx side resulted in an additional loss of 3.7 dB. The loss due to coupling from the OF to the PD was also measured to be ~2.5 dB. However, the significant loss was due to light coupling from the free space channel to the OF, which was 5 dB. This additional loss of 11.2 dB will result in unavailability of the link even under the clean channel. Note that, in order to

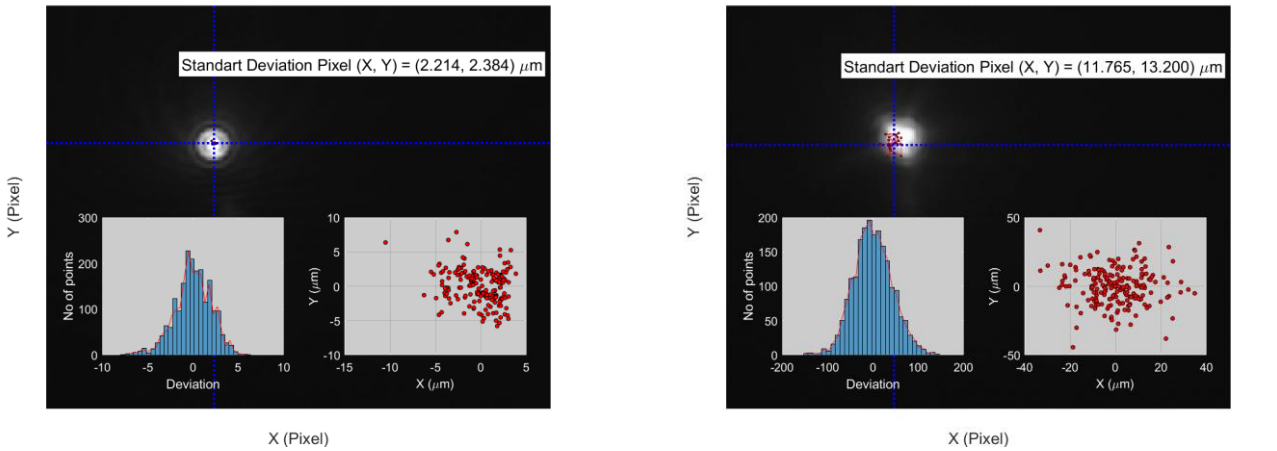

Fig. 5: Stability of focused beam at Rx for: a) clear channel, and b) turbulent channel with $C_n^2 = 2.22\times10^{-10}\ m^{-2/3}$. The inset plots are showing scatter plot as well as histogram distribution of the beam position.

compensate for the link loss an optical amplifier is used to boost the light level (i.e., higher SNR).

In this work, we have used a 1 mm core size MMF at the Rx, thus a larger field of view, which is beneficial under turbulence induced beam wandering. To investigate the effect of turbulence on the focused beam at Rx, we replaced the Rx fibre port with a camera located 8 cm behind the eyepiece lens and recorded the focused beam scattering under both clear and turbulence conditions for 3 minutes with a frame rate of 11 frames per second, see Fig. 4(e). The recorded images were then processed to determine the beam stability with the results shown in Fig. 5. The figure also shows the scatter plot as well as the histogram distributions of the beam position, which is Gaussian [16]. Comparing the beam stability in clear and turbulence channels, see Fig. 5(a) and (b), the beam scattering is < 1 mm core OF. The standard deviation of beam location for the clear and turbulence channels were measured to be 7.26 and 42.54 μm, respectively. Note that, to reduce the effect of beam scattering at the Rx, this increase the received optical power level and improves the SNR, one could use a concave mirror with the optical Rx (or OF) located at its focal point as we demonstrated in our earlier work in [17].

In fact, the low level of deviation (i.e., scattering) showed that, a MMF with a core size of 52 or 62.5 μm can be used, which will need very careful alignment. Note that, the size of the core is also decided based on the focused beam spot size. If the beam radius at the fibre port is R, the radius of focused spot is given by [18, 19]:

$$R' = \frac{\lambda f}{\pi R}, \tag{8}$$

where f is the focal length of the fibre port. Using the value of R given in Table 1, $R' \cong 0.23$ μm, which indicates that a SMF with a core size of ~10 μm can be also used to collect the focused light. However, using a small core size fibre the loss will be higher due to beam wandering and misalignment.

Note that, we have considered several conditions on the beam divergence to ensure the link's immune to the channel imperiments. As a guide to designers, in slecting the appropriate size of optic one should follow the folloing stepts: (i) based on the link distance and the turbulence levels, determine the smallest aperture size using (7); (ii) the beam size should be at least twice the Rx diameter to compensate for the pointing error, thus, the divergence angle can be determined based on the beam size and the link range; and (iii) using (1) determine the channel's geometrical loss. If the geometrical loss is higher than aceptable level, then the size of the received beam should be reduced hence changing the turbulence level.

IV. Conclusion

We proposed an experimental 1 Gbps FSO system and investigated its performance under fog and turbulence channel conditions. We outlined the sources of all additional losses incurred in link and investigated the effects of turbulence on the beam stability (i.e., beam wondering). The losses due to clipping at the transmitter and coupling from the fibre to the photodetector can be reduced by using a larger diameter fibre port and different fibre core sizes, respectively. We showed that, the most dominant loss, which needs addressing, is due to the coupling of light from the free space channel into an optical fibre at the receiver. We outlined that, the proposed link with turbulence offered almost the same data rate as a clear channel, while the packet-error-rate was downgraded from 10^{-3} to 2×10^{-2}.

Acknowledgment

This project was supported by VILIRI TSB VILIRI project (Reference: TS/R020019/), and in parts by Media Lab Asia (Sir Visvesvaraya Young Faculty Research Fellowship) under the MeitY; and Science and Engineering Research Board, Dep. of Science and Technology, Government of India, for the Project Ref. No. EMR/2016/000592.

References

[1] M. Uysal, C. Capsoni, Z. Ghassemlooy, A. Boucouvalas, and E. Udvary, *Optical Wireless Communications: An Emerging Technology*. Springer, 2016.

[2] M. Alzenad, M. Z. Shakir, H. Yanikomeroglu, and M. Alouini, "FSO-Based Vertical Backhaul/Fronthaul Framework for 5G+ Wireless Networks," *IEEE Communications Magazine*, vol. 56, no. 1, pp. 218-224, 2018.

[3] Z. Ghassemlooy, S. Rajbhandari, and W. Popoola, *Optical wireless communications: system and channel modelling with MATLAB*. Boca Raton, FL: Taylor & Francis, 2013.

[4] G. Hutton, "Full-fibre networks in the UK," CBP 8392, 2018, Available: https://researchbriefings.parliament.uk/ResearchBriefing/Summary/CBP-8392.

[5] M. P. J. Lavery, H. Huang, Y. Ren, G. Xie, and A. E. Willner, "Demonstration of a 280 Gbit/s free-space space-division-multiplexing communications link utilizing plane-wave spatial multiplexing," *Optics Letters*, vol. 41, no. 5, pp. 851-854, 2016/03/01 2016.

[6] Y. Ren *et al.*, "Experimental characterization of a 400 Gbit/s orbital angular momentum multiplexed free-space optical link over 120 m," *Optics Letters*, vol. 41, no. 3, pp. 622-625, 2016/02/01 2016.

[7] A. Prokes, "Atmospheric effects on availability of free space optics systems," 2009, vol. 48, p. 10: SPIE.

[8] *Safety of laser products - Part 1: Equipment classification and requirements*, IEC 60825-1:2001, 2001.

[9] M. M. Abadi, Z. Ghassemlooy, M. R. Bhatnagar, S. Zvanovec, M. Khalighi, and A. Maheri, "Using differential signalling to mitigate pointing errors effect in FSO communication link," in *2016 IEEE International Conference on Communications Workshops (ICC)*, 2016, pp. 145-150.

[10] M. A. Khalighi, N. Schwartz, N. Aitamer, and S. Bourennane, "Fading reduction by aperture averaging and spatial diversity in optical wireless systems," *Optical Communications and Networking, IEEE/OSA Journal of*, vol. 1, no. 6, pp. 580-593, 2009.

[11] S. M. Navidpour, M. Uysal, and M. Kavehrad, "BER performance of free-space optical transmission with spatial diversity," *Wireless Communications, IEEE Transactions on*, vol. 6, no. 8, pp. 2813-2819, 2007.

[12] M. Mansour Abadi, Z. Ghassemlooy, M. R. Bhatnagar, S. Zvanovec, M.-A. Khalighi, and M. P. J. Lavery, "Differential Signalling in Free-Space Optical Communication Systems," *Applied Sciences*, vol. 8, no. 6, p. 872, 2018.

[13] M. Ijaz, Z. Ghassemlooy, J. Pesek, O. Fiser, H. Le Minh, and E. Bentley, "Modeling of fog and smoke attenuation in free space optical communications link under controlled laboratory conditions," *Lightwave Technology, Journal of*, vol. 31, no. 11, pp. 1720-1726, 2013.

[14] M. M. Abadi, Z. Ghassemlooy, S. Zvanovec, M. R. Bhatnagar, and Y. Wu, "Hard switching in hybrid FSO/RF link: Investigating data rate and link availability," in *2017 IEEE International Conference on Communications Workshops (ICC Workshops)*, 2017, pp. 463-468.

[15] *iPerf - The ultimate speed test tool for TCP, UDP and SCTP*. Available: https://iperf.fr/

[16] A. A. Farid and S. Hranilovic, "Outage capacity optimization for free-space optical links with pointing errors," *Lightwave Technology, Journal of*, vol. 25, no. 7, pp. 1702-1710, 2007.

[17] M. Hulea, Z. Ghassemlooy, S. Rajbhandari, and X. Tang, "Compensating for Optical Beam Scattering and Wandering in

FSO Communications," *Journal of Lightwave Technology*, vol. 32, no. 7, pp. 1323-1328, 2014.

[18] B. E. A. Saleh and M. C. Teich, *Fundamentals of photonics*. New York, Chichester: Wiley, 1991.

[19] A. E. Siegman, *Lasers*. Mill Valley, Calif Oxford: University Science Books, 1986.